New concept to break the intrinsic properties of organic semiconductors for optical sensing applications

Wallace C.H. Choy
Department of Electrical and Electronic Engineering, the University of Hong Kong, Hong Kong, China
Email: chchoy@eee.hku.hk

ABSTRACT

As the intrinsic electrostatic limit, space charge limit (SCL) for photocurrent is a universal phenomenon which is fundamental important for organic semiconductors. We will demonstrate SCL breaking by a new plasmonic-electrical concept. As a proof-of-concept, organic solar cells (OSCs) comprising metallic planar and grating electrodes are studied. Interestingly, although strong plasmonic resonances induce abnormally dense photocarriers around a grating anode, the grating incorporated inverted OSC is exempt from space charge accumulation (limit) and degradation of electrical properties. The plasmonic-electrical concept will open up a new way to manipulate both optical and electrical properties of semiconductor devices simultaneously.

INTRODUCTION

The space charge limit (SCL) effect is a universal phenomenon in semiconductor devices involving light emitting diodes, solar cells, and photodetectors. Typically, the SCL will exist in the condition of (1) unbalanced hole and electron mobility; (2) thick active layer; (3) high light intensity or dense photocarriers (electrons and holes) generation; and (4) moderate reverse bias. A low mobility of hole as compared to that of electron can be occurred in organic semiconductor devices dependent on device fabrication procedures, for instance, the thermal annealing, solvent annealing, etc. In the planar-inverted organic solar cells (OSCs), photocarriers will be generated at the region close to the transparent cathode, such as indium tin oxide (ITO), where incident light will first penetrate. The photogenerated holes with a low mobility will have to transport through the whole active layer, and then reach to the anode. If the length of the active layer is longer than the mean drift length of holes, the incurred SCL can be easily observed due to the severely unbalanced mobility of electron and hole and the accumulated holes (i.e. space charges) inside the device. As a consequence, the short circuit current and fill factor of OSCs will drop significantly due to both bulk recombination and space charge formations.

In this work, through the study of plasmonic OSCs, we will show metallic nanostructures go beyond their optical functions to control recombination, transport, and collection of photocarriers generated from active organic materials. Through spatially redistributing light absorption at the active layer, the proposed plasmonic-electrical concept is fundamentally different from the hot carrier effect where photocarriers are generated from metallic nanostructures. The eliminated SCL in OSCs has been demonstrated through incorporating metallic (Ag or Au) nanostructures and then the improved efficiency is achieved [1]. Consequently, the investigation of plasmonic-electrical [2-4] and plasmonic-optical [5-9] effects can enhance device performances such as improving the light absorption of solar cells, increasing emission efficiency of light emitting devices, reducing dark current and enhancing sensitivity of photodetector as well as intensifying the surface enhanced Raman scattering for biosensor applications.

EXPERIMENTS AND RESULTS

SCL elimination in Ag-grating-inverted (hole-path shortened) OSCs

The commonly polymer blend of poly(3-hexylthiophene):[6,6]-phenyl-C61-butyric acid methyl ester (P3HT:PCBM) is used. To demonstrate the SCL effect, three structural and material configurations were fabricated to intuitively show the plasmonic-electrical effects. 1. Annealed P3HT:PCBM active layer at non-optimized annealing temperature (robust and well-recognized) for unbalanced electron/ hole mobility and low hole mobility (to favor SCL effects). 2. Inverted OSC structures for a long hole transport path (to favor SCL effects). 3. Metallic nanograting as an anode shown in Figure 1(b) for demonstrating the plasmonically modified SCL effect. The planar and grating OSCs are inverted device structures of ITO/TiO_2 (20 nm)/active layer (220 nm)/MoO_3 (10 nm)/Ag (with or without grating) (100 nm) (See Figure 1). For comparative and systematic study, the planar and grating OSCs with normal device structures of ITO/ PEDOT:PSS (30 nm)/active layer (220 nm)/Ca (10 nm)/Ag (with or without grating) (100 nm) are also fabricated. All the active layer thicknesses are about 220 nm.

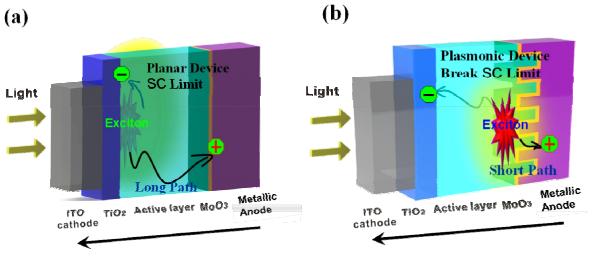

Figure 1. A schematic pattern of inverted OSC devices. (a) inverted OSCs with a planar metallic anode; (b) inverted OSCs with a grating metallic anode. The short notation "SC" denotes the space charge. A long transport path of holes in the planar-inverted OSC induces the SCL characteristics. A short transport path of holes manipulated by the plasmonic-electrical effect in the grating-inverted OSC breaks the SCL.

Infrared Remote Sensing and Instrumentation XXIII, edited by Marija Strojnik Scholl, Gonzalo Páez, Proc. of SPIE Vol. 9608, 96081A · © 2015 SPIE
CCC code: 0277-786X/15/$18 · doi: 10.1117/12.2187190

According to the Mott-Gurney law states photocurrent (J_{ph}) in the SCL regime can be described as following using negligible number of deep localized states and field independent mobility.

$$J_{ph} = \left(\frac{9\varepsilon_0\varepsilon_r\mu_h}{8}\right)^{1/4} (qG)^{3/4} V_e^{1/2} \quad (1)$$

where G, V_e, μ_h, q, $\varepsilon_0\varepsilon_r$ are the averaged generation rate, the effective voltage drop across the active layer or hole accumulation region, the hole mobility, the electron charge and the dielectric permittivity of the active layer respectively. The compensation voltage V_0, which is almost equal to the built-in potential of OSCs, is defined as $J_{ph}(V_0)=0$. The effective applied voltage V_e is given as V_0-V, where V is the applied bias voltage. Differently, under a sufficiently large reverse bias (ignorable recombination), J_{ph} is approximated as

$$J_{ph} = qGL \quad (2)$$

where L is the active layer's thickness.

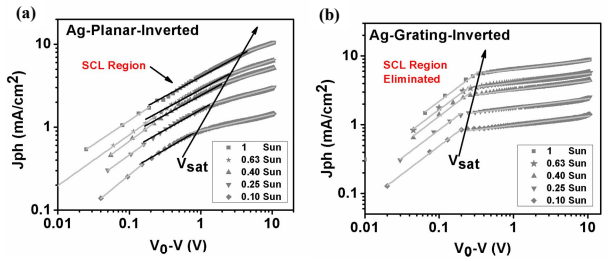

Figure 2. SCL characteristics for Ag-inverted OSCs. photocurrents versus effective applied voltage at different incident light intensities. (a) Ag-planar-inverted OSCs, and (b) Ag-grating-inverted OSCs. Light intensity is varied from 100,
63, 40, 25, to 10 mW cm^{-2} by using neutral density filters. The black solid lines in (a) represent the square-root dependence of photocurrent on effective applied voltage (SCL region).

SCL characteristics in Ag-planar-inverted and Ag-grating-inverted OSCs have been studied by measuring J_{ph} under various incident light intensity and effective applied voltage (V_0-V) conditions at room temperature and the results are shown in Figure 2**.** For the Ag-planar-inverted device, when V_0-V<0.2 V (i.e. a low internal electrostatic field, see Figure 2(a)), the approximately linear proportion of J_{ph} to V_0-V is mainly governed by the diffusion and drift currents effect. As internal field increases, J_{ph} shows a square-root dependence on V_0-V. When the internal field further increases, under sufficiently high reverse voltage, photocurrent becomes saturated (internal-field independent) with no occurrence of recombination, indicating the mean distance (w) of free charge carriers becomes equal to or larger than the active layer thickness (L). The J_{ph}'s dependence on V_0-V reveal the current transition from diffusion and drift current, to SCL limited current and finally saturated current with no occurrence of recombination. The J_{ph} versus light intensity at three different effective applied voltages (at V_0-V =0.2 V, 0.5 V, 1 V in the square-root regime, and V_0-V =10 V in the saturation regime) is extracted as shown in Figure 3 and further verify the SCL occurrence in the Ag-planar-inverted OSC. From the results for planar inverted OSCs (see Figure 3(a)), J_{ph} is approximately proportional to $I^{3/4}$ at the SCL region (1/2 power dependence of J_{ph} on V_0-V) and proportional to $I^{0.93}$ at the saturation region for sufficiently high V_0-V. According to Equation (1) and (2), we conclude that the space charge effect occurs and dominates electrical properties of the Ag-planar-inverted device.

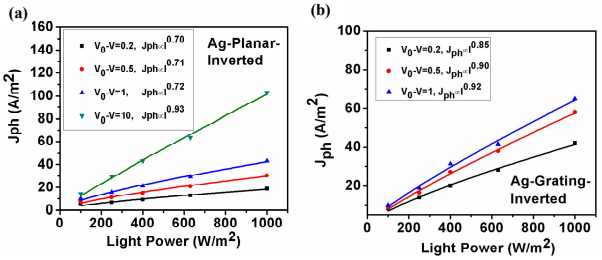

Figure 3. Photocurrents versus incident light intensity at different effective applied voltages. (a) Ag-planar-inverted OSCs, and (b) Ag-grating-inverted OSCs.

Regarding the Ag-grating-inverted OSCs, J_{ph} versus V_0-V at different incident light intensities is shown in Figure 3(b). Amazingly, the SCL characteristics disappear when a metallic grating anode is incorporated. When V_0-V <0.2 V, J_{ph} is almost linearly proportional to V_0-V, which is the same as the Ag-planarinverted device. However, at higher voltages, J_{ph} becomes saturated and shows no square-root dependence on V_0-V. Furthermore, extracting the curve of J_{ph} versus the light intensity at different V_0-V, J_{ph} shows a linear dependence on the light intensity. This suggests the eliminated SCL and reduced bulk recombination.

SCL characteristics in normal (electron-path shortened) OSCs

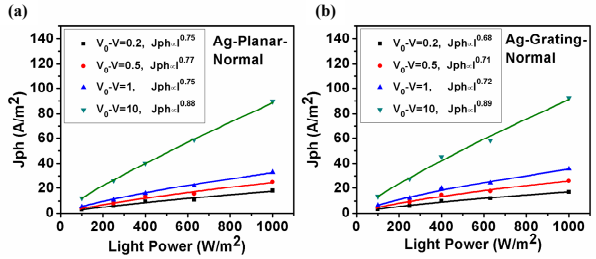

Figure 4. Photocurrents versus incident light intensity at different effective applied voltages. (a) Ag-planar-noral OSCs, and (c) Ag-grating-inverted OSCs.

Differently, in the normal devices, the Ag grating as a cathode for collecting electrons and electrons (not holes) transport a short path before collected by the cathode. For both Ag-planar normal and Ag-grating-normal devices, we study J_{ph} versus V_0-V at different incident light intensities and J_{ph} versus light intensity at four different V_0-V. (Figures 4) At the square-root region of J_{ph}, photocurrent is approximately proportional to $I^{3/4}$. Particularly, the Ag-grating-normal device shows the same SCL characteristics at room temperature as what the Ag-planar-normal device does. The short transport path of high-mobility electrons does not reduce charge accumulation and thus SCL

still exists. To improve electrical properties of OSCs, the device architecture with metallic nanostructures should be carefully engineered to redistribute light absorption for shortening the transport path of low-mobility photocarriers

Space charge dependent OSC performances.

Electrical characteristic parameters of OSCs with four different device structures are listed in Table 1. For the Ag-normal OSCs, the characteristic parameters including shortcircuit current (J_{SC}) and fill factor (FF) show no significant distinction for both planar and grating devices. After introducing the nanostructured cathode, the increased J_{SC} and reduced FF are respectively due to the metallic grating enhanced optical absorption and elongated hole (shortened electron) transport path. However, for the Ag-inverted OSCs, the characteristic parameters of the planar and grating devices show considerable differences. For example, FF of the Ag-planar-inverted device drops drastically compared to that of Ag-grating-inverted one. The maximum possible FF at the SCL regime is about 42%. From results in Table 1, FF of the Ag-planar-inverted and Ag-grating-inverted devices are respectively lower and higher than 42%. The OSCs, which achieve a FF significantly larger than 42%, will be exempt from the SCL. The FF of the Ag-planar-inverted device is noticeably smaller than 42% due to the SCL effect with a large recombination loss. Furthermore, J_{SC} of the Ag-grating-inverted device is improved by 75% in comparison with the Ag planar-inverted one. On one hand, surface plasmons excited in the metallic grating enhance the optical absorption of OSCs. On other hand, low-mobility holes, abnormally generated around the grating anode, are collected fast and easily leading to the reduced recombination loss. Hence, the Ag-grating-inverted device improves J_{SC} much more significantly than the Ag-grating-normal one, although the same optical enhancement can be achieved by the Ag-grating-normal device. Considering the improved FF together with the boosted short-circuit current, the PCE of the Ag-gratinginverted device increases from 0.73% to 1.73%.

Device	V_{OC} (V)	J_{SC} (mA/cm^2)	FF (%)	PCE (%)
Ag-Planar-Inverted	0.61±0.02	3.30±0.15	37±2	0.73±0.10
Ag-Grating-Inverted	0.61±0.01	5.76±0.28	56±5	1.73±0.21
Ag-Planar-Normal	0.61±0.01	2.73±0.25	44±2	0.74±0.10
Ag-Grating-Normal	0.61±0.02	2.98±0.21	41±3	0.75±0.21

Table 1. Experimental characteristic parameters of OSCs with different structures. The parameters include open-circuit voltage (V_{OC}), short circuit current (J_{SC}), fill factor (FF), and power conversion efficiency (PCE).

Conclusion

In conclusion, the work demonstrated the plasmonic-electrical effect breaks the SCL in inverted OSCs through introducing a metallic nanostructured anode. The linear dependence of photocurrent on light intensity and significantly improved FF are clear proofs for the eliminated SCL characteristics. Plasmonically induced light absorption redistribution shortens the transport path of low-mobility holes; and thus reduces bulk recombination and space charge accumulation. Consequently, exploiting both plasmonic-optical and plasmonic-electrical effects via metallic nanostructures will open up a more flexible and integrated way to design high-performance optoelectronic nanodevices.

Acknowledgements

The work is supported by the University Grant Council of the University of Hong Kong (grant #201311159056, 201411159040), the General Research Fund (grants HKU711813 and HKU711612E), the Collaborative Research Fund (grant C7045-14E) and RGC-NSFC grant (N_HKU709/12) from the Research Grants Council of Hong Kong Special Administrative Region, China, and grant CAS14601 from CAS-Croucher Funding Scheme for Joint Laboratories and the Collaborative Research grant from the research grant council of Hong Kong (CUHK1/CRF/12G).

References

[1] W.E.I. Sha, X. Li, W.C.H. Choy, Scientific Reports, vo l. 4, p. 6236 (10pp), 2014.
[2] F.X. Xie, W.C.H. Choy, W.E.I. Sha, D. Zhang, S. Zhan g, X. Li, C.W. Leung, J. Hou, Energy Environ. Sci., vol. 6, pp.3372 – 3379, 2013;
[3] D. Zhang, W.C.H. Choy, F. Xie, W.E.I. Sha, X. Li, B. Ding, K. Zhang, F. Huang, and Y. Cao, Adv. Funct. Mat., vol. 23, pp.4255–4261, 2013;
[4] D.D.S. Fung, L. Qiao, W.C.H. Choy, C.C.D. Wang, W. E.I. Sha, F. Xie, and S. He, J. Mater. Chem., vol. 21, pp. 1 6349 – 16356, 2011.
[5] X.H. Li, W.C. H. Choy, X. Ren, D. Zhang, H.F. Lu, A dv. Funct. Mat. vol. 24, pp. 3114 - 3122, 2014.
[6] X.H.Li, W.C.H.Choy, H.F. Lu, W.E.I. Sha, and H. P. H o, Adv. Funct. Mat., vol.23, pp.2728–2735, 2013;
[7] X.H. Li, W. C.H. Choy, L Huo, F.X. Xie, W.E.I. Sha, B. Ding, X. Guo, Y. Li, J. Hou, J. You, Y. Yang, Adv. Mate r. vol. 24, pp.3046-3052, 2012;
[8] X.H. Li, W. E.I. Sha, W.C.H. Choy, D.D.S. Fung, F. X. Xie, J. of Phys. Chem. C, vol. 116, pp.7200-7206, 2012;
[9] C.C.D. Wang, W. C. H. Choy, C. Duan, D.D.S. Fung, W.E.I. Sha, F.X. Xie, F. Huang, and Y. Cao, J. Mater. Che m., vol. 22, pp.1206–1211, 2012.